Trabajos Fin de Grado

Cómo hacer un documento científico

José María Martín Olalla
olalla@us.es; @MartinOlalla_JM

Departamento de Física de la Materia Condensada
Universidad de Sevilla

Grado en Física

Partes de un trabajo científico

IMRAD

1. Título.
2. Autor y filiación.
3. Resumen (abstract).
4. Introducción.
5. Metodología.
6. Resultados.
7. Discusión.
8. Conclusiones.
9. Bibliografía.

Elementos particulares

1. Estilo.
2. Figuras.
   - Gráficas. (`gnuplot`, `matplotlib`)
   - Esquemas. (`Xfig`,`inkscape`)
3. Cuadros de datos.
4. Fórmulas matemáticas.
5. Referencias cruzadas. (BibTeX, RefTeX, `mendeley`)

Índice

Reglas de oro

1. Su trabajo va a ser revisado por otra persona.
2. Escriba, guarde en un cajón, relea y revise con intensidad y espíritu crítico.
3. Reforme: las cosas se pueden decir de varias maneras: encuentre la adecuada.
4. La importancia de la primera oración del primer párrafo de la primera sección de la primera página.
5. La importancia del primer párrafo de la primera sección de la primera página.
6. KISS: Keep It Simple, Stupid.
7. Make everything as simple as possible, but not simpler.
8. Sea consistente para que su texto sea autoconsistente:
   - Tiempo verbal.
   - Persona.
   - Símbolos.
   - Tipos de letra.
9. Sea pulcro.

Un texto científico no se escribe para que lo lea el autor

The following proof, directly quoted from a sophomore term paper, is mathematically correct (except for a minor slip) but stylistically atrocious:

$L(C,P) \subset A_n$

$C \subset L \Rightarrow C \subset A_n$

Spse $p \in P,\ p \notin A_n \Rightarrow p_i < p_j$ for $i < j$

$c + p \in L \subset A_n$

$\therefore\ c_i + p_i \geq c_j + p_j$ but $c_i \geq c_j \geq 0, p_j \geq p_i \therefore\ (c_i - c_j) \geq (p_j - p_i)$

but $\exists$ a constant $k \ni c + kp \notin A_n$

let $k = (c_i - c_j) + 1 \qquad c + kp \in L \subset A_n$

$\therefore\ c_i + kp_i \geq c_j + kp_j \Rightarrow (c_i - c_j) \geq k(p_j - p_i)$

$\Rightarrow k - 1 \geq k \cdot m \qquad k, m \geq 1 \qquad$ Contradiction

$\therefore\ p \in A_n$

$\therefore\ L(C,P) \subset A_n \Rightarrow C, P \subset A_n$ and the

lemma is true.

Imagen: Knuth, Larrabee y Roberts (1987, http://bit.ly/1UwxpAU, p. 7)

Figura 3.1.1: Ejemplo de texto (demostración) «atroz» «perpretado» por un estudiante de segundo curso en alguna universidad americana y citado por Donald Knuth.[8]

Hágase con un cierto «gusto»

A possible way to improve the quality of the writing:

Let N denote the set of nonnegative integers, and let

$$N^n = \{\, (b_1, \ldots, b_n) \mid b_i \in N \text{ for } 1 \le i \le n \,\}$$

be the set of n-dimensional vectors with nonnegative integer components. We shall be especially interested in the subset of "nonincreasing" vectors,

$$A_n = \{(a_1, \ldots, a_n) \in N^n \mid a_1 \ge \cdots \ge a_n\}\,. \tag{1}$$

If C and P are subsets of N^n, let

$$L(C, P) = \{c + p_1 + \cdots + p_m \mid c \in C, m \ge 0, \text{ and } p_j \in P \text{ for } 1 \le j \le m\} \tag{2}$$

be the smallest subset of N^n that contains C and is closed under the addition of elements of P. Since A_n is closed under addition, $L(C, P)$ will be a subset of A_n whenever C and P are both contained in A_n. We can also prove the converse of this statement.

Lemma 1. *If $L(C, P) \subseteq A_n$ and $C \neq \emptyset$, then $C \subseteq A_n$ and $P \subseteq A_n$.*

Proof. (Now it's your turn to write it up beautifully.)

Imagen: Knuth, Larrabee y Roberts (1987, http://bit.ly/1UwxpAU, p. 7)

Figura 3.1.2: Mejoras introducidas por Knuth a un texto «atroz» (véase la Fig. 3.1.1).[8]

Cuidado con las introducciones y los pie de página

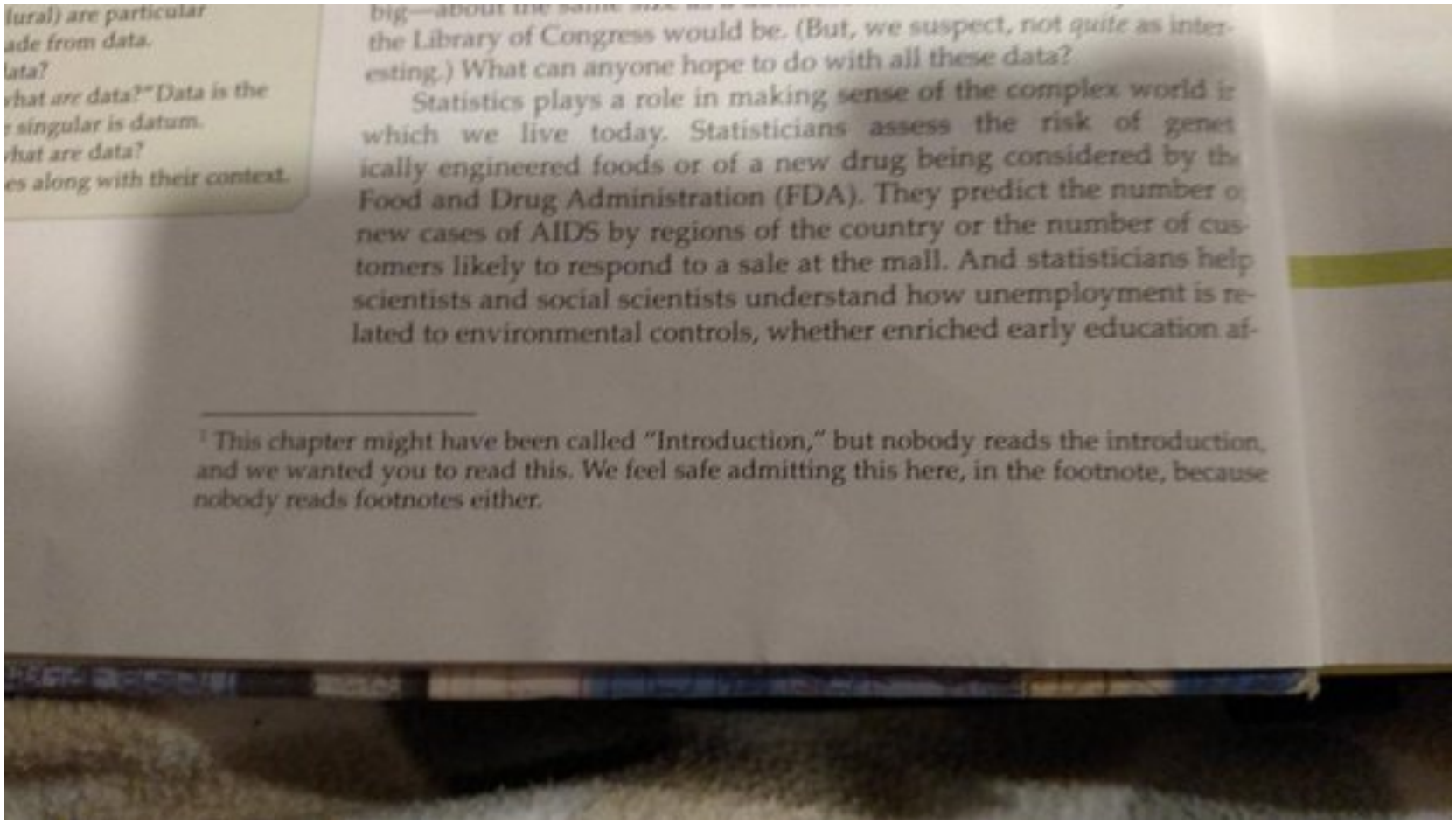

lural) are particular
ade from data.
ata?
hat are data?" Data is the
singular is datum.
hat are data?
es along with their context.

big—about the same size as a [illegible]
the Library of Congress would be. (But, we suspect, not quite as interesting.) What can anyone hope to do with all these data?

Statistics plays a role in making sense of the complex world in which we live today. Statisticians assess the risk of genetically engineered foods or of a new drug being considered by the Food and Drug Administration (FDA). They predict the number of new cases of AIDS by regions of the country or the number of customers likely to respond to a sale at the mall. And statisticians help scientists and social scientists understand how unemployment is related to environmental controls, whether enriched early education af-

[1] This chapter might have been called "Introduction," but nobody reads the introduction, and we wanted you to read this. We feel safe admitting this here, in the footnote, because nobody reads footnotes either.

Imagen: (@AcademiaObscura) (2016, http://bit.ly/22H2q9C,)

Figura 3.1.3: Este capítulo debió llamarse «Introducción» pero nadie las lee y queríamos que usted la leyera. Admitimos con tranquilidad esto aquí, en un pie de página, porque tampoco nadie lee los pie de página.[10]

"This sentence has five words. Here are five more words. Five-word sentences are fine. But several together become monotonous. Listen to what is happening. The writing is getting boring. The sound of it drones. It's like a stuck record. The ear demands some variety. Now listen. I vary the sentence length, and I create music. Music. The writing sings. It has a pleasant rhythm, a lilt, a harmony. I use short sentences. And I use sentences of medium length. And sometimes, when I am certain the reader is rested, I will engage him with a sentence of considerable length, a sentence that burns with energy and builds with all the impetus of a crescendo, the roll of the drums, the crash of the cymbals —sounds that say listen to this, it is important." (Gary Provst)

«Esta frase tiene cinco palabras. Aquí van otras cinco más. Oraciones de cinco palabras agradan. Pero muchas juntas son monótonas. Atienda a lo que ocurre. La escritura se vuelve aburrida. Es un sonido que martillea. Es como un disco rayado. El oído necesita más variedad. Ahora atienda. Varío la longitud de la oración y creo música. Música. La escritura canta. Tiene un ritmo agradable, una cadencia, una armonía. Y uso frases cortas. Y también frases de longitud media. Y, a veces, cuando estoy seguro de que el lector está tranquilo, le endiño con una frase de longitud considerable, una oración que arde con energía y emerge con todo el ímpetu de un crescendo, del redoblar de tambores, del rugir de los timbales —sonidos que dicen: atienda, esto es importante.»

Índice

Las figuras son fundamentales: primer ejemplo

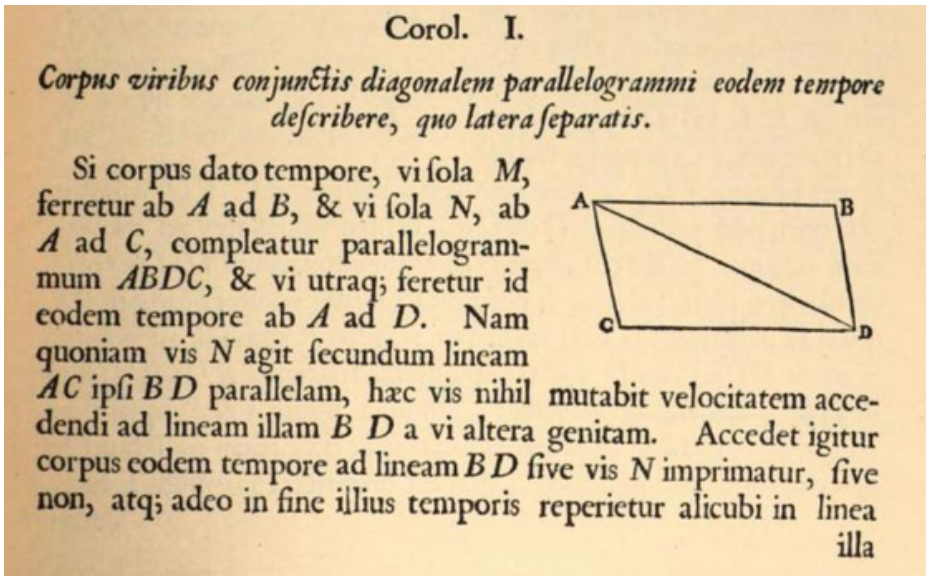

Corol. I.

Corpus viribus conjunctis diagonalem parallelogrammi eodem tempore describere, quo latera separatis.

Si corpus dato tempore, vi sola *M*, ferretur ab *A* ad *B*, & vi sola *N*, ab *A* ad *C*, compleatur parallelogrammum *ABDC*, & vi utraq; feretur id eodem tempore ab *A* ad *D*. Nam quoniam vis *N* agit secundum lineam *AC* ipsi *BD* parallelam, hæc vis nihil mutabit velocitatem accedendi ad lineam illam *BD* a vi altera genitam. Accedet igitur corpus eodem tempore ad lineam *BD* sive vis *N* imprimatur, sive non, atq; adeo in fine illius temporis reperietur alicubi in linea illa

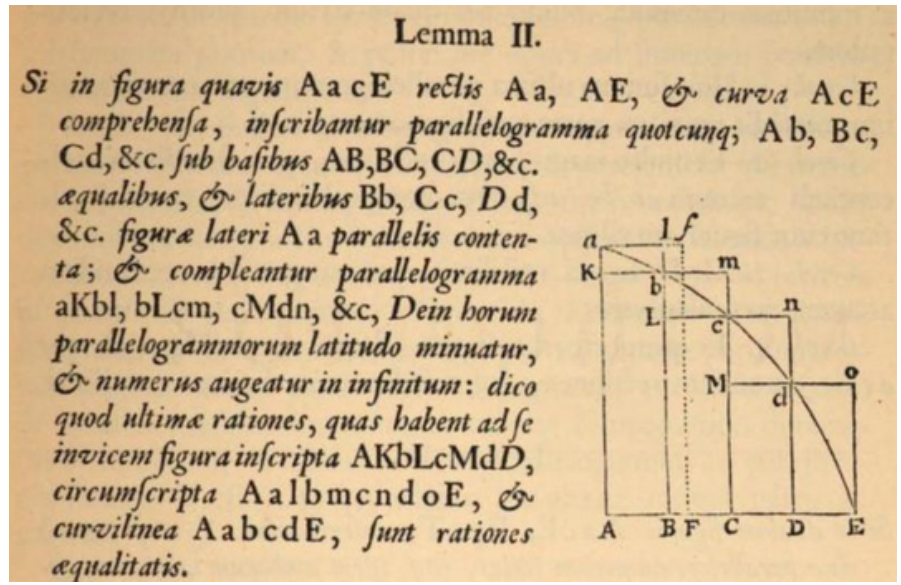

Lemma II.

Si in figura quavis AacE *rectis* Aa, AE, *& curva* AcE *comprehensa, inscribantur parallelogramma quotcunq;* Ab, Bc, Cd, &c. *sub basibus* AB,BC, CD,&c. *æqualibus, & lateribus* Bb, Cc, Dd, &c. *figuræ lateri* Aa *parallelis contenta; & compleantur parallelogramma* aKbl, bLcm, cMdn, &c, *Dein horum parallelogrammorum latitudo minuatur, & numerus augeatur in infinitum: dico quod ultimæ rationes, quas habent ad se invicem figura inscripta* AKbLcMdD, *circumscripta* AalbmcndoE, *& curvilinea* AabcdE, *sunt rationes æqualitatis.*

Imagen: Newton (1687, http://bit.ly/1ZFuAg3, pp 13 y 27)

Figura 3.2.1: Dos esquemas de *Philosophiae naturalis principia mathematica*. A la izquierda el primer ejemplo de composición de fuerzas. A la derecha el primer ejemplo de cuadratura.

Las figuras son fundamentales: segundo ejemplo

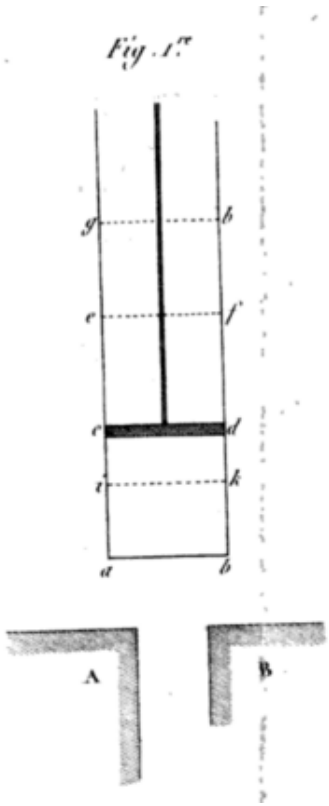

(38)

moins tous ceux qui sont propres à réaliser la puissance motrice de la chaleur. Ainsi nous sommes conduits à établir la proposition générale que voici :

La puissance motrice de la chaleur est indépendante des agens mis en œuvre pour la réaliser; sa quantité est fixée uniquement par les températures des corps entre lesquels se fait en dernier résultat le transport du calorique.

Imagen: Carnot (1824, , p 38)

Figura 3.2.2: A la izquierda, primera figura de *Réflexions sur le puissance motrice du feu, et sur les machines propes á dèveloper cette puissance* con el esquema de un pistón y sus transformaciones a lo largo de sucesivos procesos. El esquema sirve para desarrollar el principio de Carnot a la derecha.

Las figuras son fundamentales: tercer ejemplo

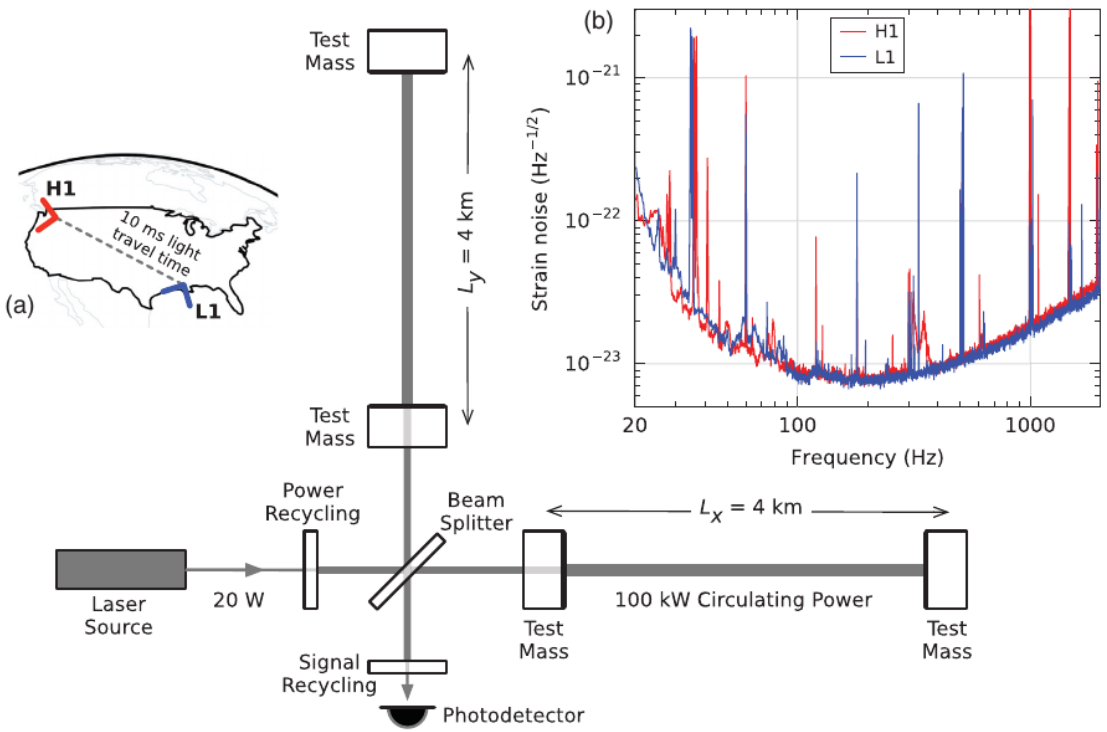

FIG. 3. Simplified diagram of an Advanced LIGO detector (not to scale). A gravitational wave propagating orthogonally to the detector plane and linearly polarized parallel to the 4-km optical cavities will have the effect of lengthening one 4-km arm and shortening the other during one half-cycle of the wave; these length changes are reversed during the other half-cycle. The output photodetector records these differential cavity length variations. While a detector's directional response is maximal for this case, it is still significant for most other angles of incidence or polarizations (gravitational waves propagate freely through the Earth). *Inset (a):* Location and orientation of the LIGO detectors at Hanford, WA (H1) and Livingston, LA (L1). *Inset (b):* The instrument noise for each detector near the time of the signal detection; this is an amplitude spectral density, expressed in terms of equivalent gravitational-wave strain amplitude. The sensitivity is limited by photon shot noise at frequencies above 150 Hz, and by a superposition of other noise sources at lower frequencies [47]. Narrow-band features include calibration lines (33–38, 330, and 1080 Hz), vibrational modes of suspension fibers (500 Hz and harmonics), and 60 Hz electric power grid harmonics.

Imagen: Abbott y col. (2016, http://bit.ly/1UQoCsR, p 4)

Figura 3.2.3: Esquema reciente de un dispositivo experimental con su pie explicativo.[3]

Las gráficas son un tipo de figura

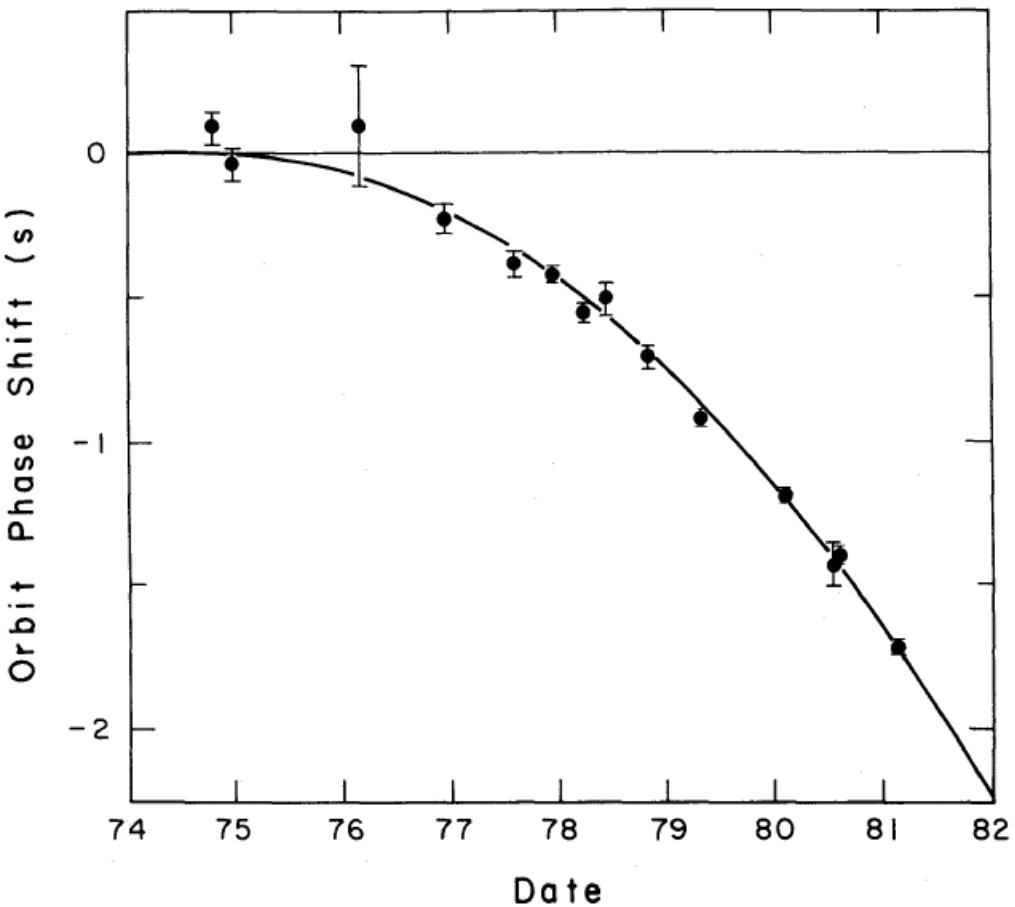

FIG. 6.—Orbital phase residuals, obtained from the data listed in Table 4. If the orbital period had remained constant, the points would be expected to lie on a straight line. The curvature of the parabola drawn through the points corresponds to the general relativistic prediction for loss of energy to gravitational radiation, or $\dot{P}_b = -2.40 \times 10^{-12}$.

Figura 3.2.4: Figura obtenida de un artículo publicado en el 1982.[4]

Imagen: Taylor y Weisberg (1982, , p 916)

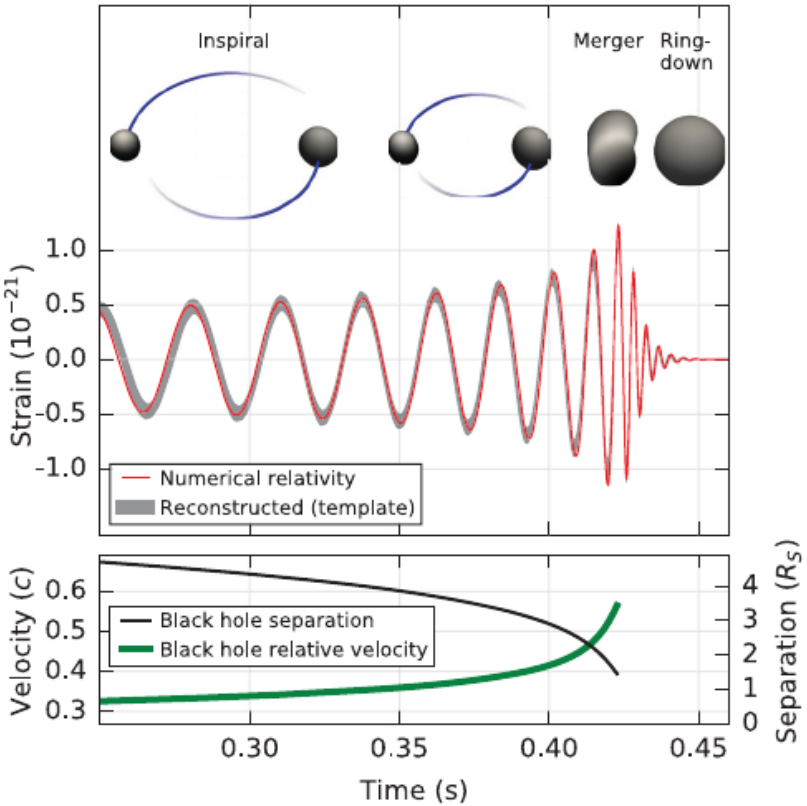

FIG. 2. *Top:* Estimated gravitational-wave strain amplitude from GW150914 projected onto H1. This shows the full bandwidth of the waveforms, without the filtering used for Fig. 1. The inset images show numerical relativity models of the black hole horizons as the black holes coalesce. *Bottom:* The Keplerian effective black hole separation in units of Schwarzschild radii ($R_S = 2GM/c^2$) and the effective relative velocity given by the post-Newtonian parameter $v/c = (GM\pi f/c^3)^{1/3}$, where f is the gravitational-wave frequency calculated with numerical relativity and M is the total mass (value from Table I).

Imagen: Abbott y col. (2016, `http://bit.ly/1UQoCsR`, p 3)

Figura 3.2.5: Ejemplo reciente de figura y pie de figura. El énfasis no está en el original.

Pie de figura Descripción autoconsistente de la figura.

Elementos de una gráfica Ejes.
Etiquetas de los ejes.
Marcas de los ejes.

Índice

El arte de escribir fórmulas y símbolos matemáticos

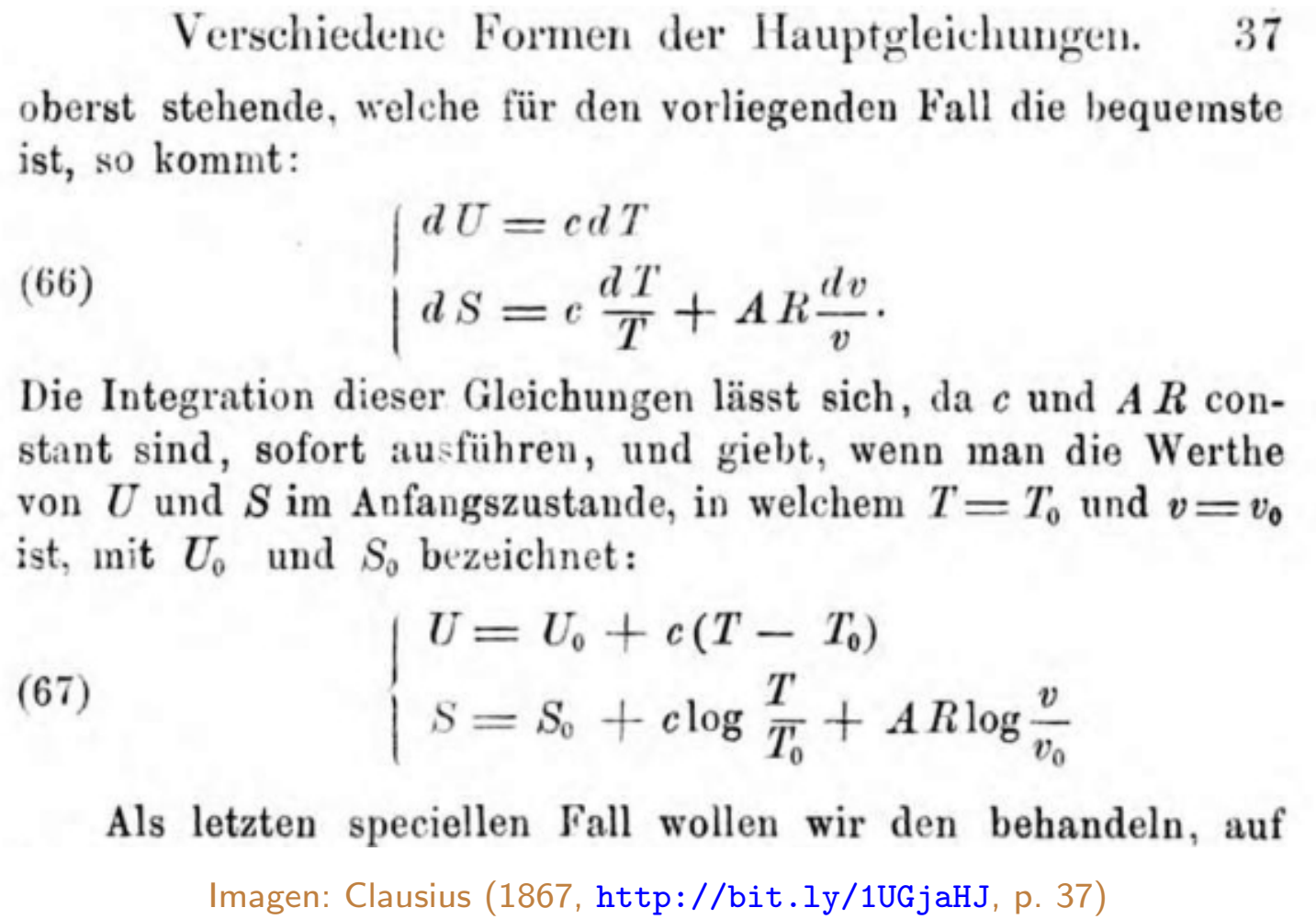

Verschiedene Formen der Hauptgleichungen. 37

oberst stehende, welche für den vorliegenden Fall die bequemste ist, so kommt:

$$(66)\qquad \left|\begin{array}{l} dU = c\,dT \\ dS = c\,\dfrac{dT}{T} + AR\dfrac{dv}{v}. \end{array}\right.$$

Die Integration dieser Gleichungen lässt sich, da c und AR constant sind, sofort ausführen, und giebt, wenn man die Werthe von U und S im Anfangszustande, in welchem $T = T_0$ und $v = v_0$ ist, mit U_0 und S_0 bezeichnet:

$$(67)\qquad \left|\begin{array}{l} U = U_0 + c(T - T_0) \\ S = S_0 + c\log\dfrac{T}{T_0} + AR\log\dfrac{v}{v_0} \end{array}\right.$$

Als letzten speciellen Fall wollen wir den behandeln, auf

Imagen: Clausius (1867, http://bit.ly/1UGjaHJ, p. 37)

Figura 3.3.1: Ejemplo de fórmulas matemáticas del siglo XIX y que contiene casi todas las convenciones que aún hoy en día se usan.[5]

Convenciones

- Variables en letra cursiva: T, t, h
- Unidades en letra redonda:

$$m = 2m \text{ y } m \neq 0 \Longrightarrow 1 = 2 \text{ (absurdo)},$$

$$m = 2\,\mathrm{m} \Longrightarrow \text{ ok.}$$

- Funciones matemáticas en letra redonda: $\log x \neq logx$.
- ¿El castellano en las funciones? Mmm, no siempre: $\sin(x)$ no $\mathrm{sen}(x)$.
- Las fórmulas forman parte de una oración: se puntúan. Véase la Fig. 3.3.1.
- Los símbolos se definen en su primera aparición:
  - Postpuestos (más normal en un contexto físico): «la presión p es entonces la fuerza por unidad de superficie».
  - Prepuestos (más normal en un contexto matemático o tras una fórmula): «sea p un número primo» o «donde p es la presión, c es una constante...»
- No hace falta definir símbolos muy usados: π, e o t como símbolo del tiempo.
- Normalmente las magnitudes exigen un complemento específico: «donde T es la temperatura del cuerpo» o «donde m es la masa de la partícula puntual».

Índice

Table de la chaleur spécifique des gaz.

NOMS DES GAZ.	Chal. spéc. sous pression constante.	Chal. spéc. sous volume constant.
Air atmosphérique.	1,000	0,700
Gaz hydrogène.	0,903	0,603
Acide carbonique.	1,258	0,958
Oxigène.	0,976	0,676
Azote.	1,000	0,700
Protoxide d'azote.	1,350	1,050
Gaz oléfiant.	1,553	1,253
Oxide de carbone.	1,034	0,734

Les nombres de la première colonne et ceux de la seconde sont ici rapportés à la même unité, à la chaleur spécifique de l'air atmosphérique sous pression constante.

Figura 3.4.1: Cuadro con los valores de los calores específicos a presión y volumen constante para diferentes gases. El cuadro está insertado en el texto y el párrafo posterior lo describe.[2]

Imagen: Carnot (1824, ,)

Un ejemplo reciente y simple

TABLE I. Source parameters for GW150914. We report median values with 90% credible intervals that include statistical errors, and systematic errors from averaging the results of different waveform models. Masses are given in the source frame; to convert to the detector frame multiply by $(1+z)$ [90]. The source redshift assumes standard cosmology [91].

Primary black hole mass	$36^{+5}_{-4} M_\odot$
Secondary black hole mass	$29^{+4}_{-4} M_\odot$
Final black hole mass	$62^{+4}_{-4} M_\odot$
Final black hole spin	$0.67^{+0.05}_{-0.07}$
Luminosity distance	410^{+160}_{-180} Mpc
Source redshift z	$0.09^{+0.03}_{-0.04}$

Imagen: Abbott y col. (2016, http://bit.ly/1UQoCsR, p. 7)

Figura 3.4.2: Cuadro con los valores de los calores específicos a presión y volumen constante para diferentes gases. El cuadro está insertado en el texto y el párrafo posterior lo describe.[2]

Un ejemplo más complicado

TABLE 1

PARAMETERS OF OBSERVING SYSTEMS USED FOR PSR 1913+16

Dates	Frequency (MHz)	Total Bandwidth (MHz)	Frequency Channels	Number of Polarizations	System Noise Temp. (K)	Recording Method[a]	Time Resolution (μs)	RMS Measurement Uncertainty (μs)	Number of Observations	Nominal Assigned Weight
A. 1974 Sep–Dec	430	8.0	32	2	175	FS	5000	275	524	0.04
B. 1975 Apr–1976 Nov	430	0.64 or 3.2	32	1 or 2	175	AVG	2000	310	112	0.01
C. 1975 Jun–1976 Feb	430	0.25	1	2	175	AVG	2000	890	75	0.001
D. 1976 Nov–Dec.....	430	0.64	32	1	175	FS	750	155	73	0.1
E. 1977 Jul–Aug	430	0.64	32	1	175	AVG	340	150	52	0.1
F. 1978 Jun–1981 Feb	430	3.34	504	2	175	AVG	43	75	572	1.0
G. 1977 Jul–Aug.....	1410	8.0	32	2	80	AVG	125	75	57	0.2
H. 1977 Dec	1410	8.0	32	2	80	AVG	125	55	45	0.6
I. 1978 Mar–Apr.....	1410	8.0	32	2	80	FS	125	50	120	1.0
J. 1980 Jul–1981 Feb	1410	8.0	32	2	80, 40	AVG	200	85	312	1.0
K. 1981 Feb–Mar.....	1410	16.0	64	2	40	AVG	125	25	415	2.0

[a]FS means fast-sampled raw data were recorded on magnetic tape, with timing information; AVG means synchronous signal averaging was done at the time of observation, using a precomputed ephemeris.

Imagen: Taylor y Weisberg (1982, , p 909)

Figura 3.4.3: Cuadro con los parámetros de once observaciones realizadas sobre el pulsar PSR 1913+16. El cuadro fluye aparte del texto.[4]

Índice

Estilo alfabético

and the reconstructed x-ray temporal profile are shown in (b) and (d), respectively. From Marinelli *et al.*, 2015.

(Allaria *et al.*, 2013a). The color separation is limited by the gain bandwidth and the two pulses are separated in wavelength and in time between 300 and 700 fs.

A new scheme for the generation of ultrashort pulse trains in an FEL uses the emission from a multipeaked electron energy distribution (Petrillo *et al.*, 2013). Two electron beamlets with energy difference larger than the FEL parameter are generated by illuminating the cathode with two ps-spaced laser pulses, followed by a rotation of the longitudinal phase space by velocity bunching in the linac. The resulting SASE FEL radiation shows a double-peaked spectrum and a temporally modulated pulse structure.

A similar method was successfully developed at LCLS at x-ray energies, with the generation of two electron bunches separated in energy and time using a double laser pulse at the cathode (Marinelli *et al.*, 2015), as shown in Fig. 50. The final energy difference and time separation between the two bunches when they enter the undulator are determined by the initial time separation at the cathode and the compression applied using two magnetic chicanes during the acceleration. The two bunches generate different colors, and their separation can be much larger than the FEL bandwidth. The advantage of this scheme over previously developed methods is that the x rays can be amplified to saturation, improving the peak power by an order of magnitude with respect to other methods developed at hard x rays. Filtering the two colors through the hard x-ray self-seeding crystal (Amann *et al.*, 2012; Lutman *et al.*, 2014) gives a two-color spectrum with narrow bandwidth.

ACKNOWLEDGMENTS

C. P. thanks the SLAC National Accelerator Laboratory for its kind hospitality during the time this paper was written and acknowledges the support of DOE Grant No. DE-SC0009983. We thank many colleagues, among them R. Bonifacio, M. Cornacchia, W. Fawley, G. Geloni, R. Hettel, Z. Huang, K.-J. Kim, J. B. Murphy, H.-D. Nuhn, J. Rosenzweig, J. Rossbach, E. Saldin, A. M. Sessler, H. Winick, and M. Yurkov for the many useful discussions, over many years, providing important insight on the physics of FELs.

REFERENCES

Ackermann, W., *et al.*, 2007, Nat. Photonics **1**, 336.
Alferov, D. F., Y. A. Bashmakov, and E. G. Bessonov, 1974, Sov. Phys. Tech. Phys. **18**, 1337.
Allaria, E., *et al.*, 2012a, Nat. Photonics **6**, 699.
Allaria, E., *et al.*, 2012b, New J. Phys. **14**, 113009.
Allaria, E., *et al.*, 2013a, Nat. Photonics **7**, 913.
Allaria, E., *et al.*, 2013b, Nat. Commun. **4**, 2476.
Altarelli, M., *et al.*, 2006, The European X-ray Free-electron Laser Technical Design Report, DESY Report No. 2006-097.
Amann, J., *et al.*, 2012, Nat. Photonics **6**, 693.
Ames, W. F., 1977, *Numerical Methods for Partial Differential Equations* (Academic Press, New York).
Ayvazyan, V., *et al.*, 2002, Phys. Rev. Lett. **88**, 104802.
Becker, W., and J. K. McIver, 1983, Phys. Rev. A **28**, 1838.
Becker, W., and M. S. Zubairy, 1982, Phys. Rev. A **25**, 2200.
Ben-Zvi, I., K. M. Yang, and L. H. Yu, 1992, Nucl. Instrum. Methods Phys. Res., Sect. A **318**, 726.
Bertolotti, M., 2005, *History of the Laser* (Institute of Physics Publishing, Bristol).
Best, R. W. B., and B. Faatz, 1990, J. Phys. D **23**, 1337.
Biedron, S. G., *et al.*, 2001, Nucl. Instrum. Methods Phys. Res., Sect.

Imagen: Pellegrini, Marinelli y Reiche (2016, http://bit.ly/1ZGfgzA, p. 52)

Estilo numérico

I. INTRODUCTION

In 1916, the year after the final formulation of the field equations of general relativity, Albert Einstein predicted the existence of gravitational waves. He found that the linearized weak-field equations had wave solutions: transverse waves of spatial strain that travel at the speed of light, generated by time variations of the mass quadrupole moment of the source [1,2]. Einstein understood that gravitational-wave amplitudes would be remarkably small; moreover, until the Chapel Hill conference in 1957 there was significant debate about the physical reality of gravitational waves [3].

Also in 1916, Schwarzschild published a solution for the field equations [4] that was later understood to describe a black hole [5,6], and in 1963 Kerr generalized the solution to rotating black holes [7]. Starting in the 1970s theoretical work led to the understanding of black hole quasinormal modes [8–10], and in the 1990s higher-order post-Newtonian calculations [11] preceded extensive analytical studies of relativistic two-body dynamics [12,13]. These advances, together with numerical relativity breakthroughs in the past decade [14–16], have enabled modeling of binary black hole mergers and accurate predictions of their gravitational waveforms. While numerous black hole

[1] A. Einstein, Sitzungsber. K. Preuss. Akad. Wiss. **1**, 688 (1916).
[2] A. Einstein, Sitzungsber. K. Preuss. Akad. Wiss. **1**, 154 (1918).
[3] P. R. Saulson, Gen. Relativ. Gravit. **43**, 3289 (2011).
[4] K. Schwarzschild, Sitzungsber. K. Preuss. Akad. Wiss. **1**, 189 (1916).
[5] D. Finkelstein, Phys. Rev. **110**, 965 (1958).
[6] M. D. Kruskal, Phys. Rev. **119**, 1743 (1960).
[7] R. P. Kerr, Phys. Rev. Lett. **11**, 237 (1963).
[8] C. V. Vishveshwara, Nature (London) **227**, 936 (1970).
[9] W. H. Press, Astrophys. J. **170**, L105 (1971).
[10] S. Chandrasekhar and S. L. Detweiler, Proc. R. Soc. A **344**, 441 (1975).
[11] L. Blanchet, T. Damour, B. R. Iyer, C. M. Will, and A. G. Wiseman, Phys. Rev. Lett. **74**, 3515 (1995).
[12] L. Blanchet, Living Rev. Relativity **17**, 2 (2014).
[13] A. Buonanno and T. Damour, Phys. Rev. D **59**, 084006 (1999).
[14] F. Pretorius, Phys. Rev. Lett. **95**, 121101 (2005).
[15] M. Campanelli, C. O. Lousto, P. Marronetti, and Y. Zlochower, Phys. Rev. Lett. **96**, 111101 (2006).
[16] J. G. Baker, J. Centrella, D.-I. Choi, M. Koppitz, and J. van Meter, Phys. Rev. Lett. **96**, 111102 (2006).
[17] B. L. Webster and P. Murdin, Nature (London) **235**, 37 (1972).

Imagen: Abbott y col. (2016, `http://bit.ly/1UQoCsR`, pp. 1 y 9)

Estilo numérico

Introduction— In Ref. [1] we reported the detection of gravitational waves (GWs), observed on September 14, 2015 at 09:50:45 UTC by the twin instruments of the Laser Interferometer Gravitational-wave Observatory (LIGO) located at Hanford, Washington, and Livingston, Louisiana, in the USA [2, 3]. The transient signal, named GW150914, was detected with a false-alarm-probability of $< 2 \times 10^{-7}$ and has been associated with the merger of a binary system of black holes (BHs).

Here we discuss the properties of this source and its inferred parameters. The results are based on a complete analysis of the data surrounding this event. The only information from the search-stage is the time of arrival of the signal. Crucially, this analysis differs from the search in the following fundamental ways: it is coherent across the LIGO network, it uses waveform models that include the full richness of the physics introduced by BH spins, and it covers the full multidimensional parameter space of the considered models with a fine (stochastic) sampling; we also account for uncertainty in the calibration of the measured strain.

In general relativity, two objects in orbit slowly spiral together due to the loss of energy and momentum through gravitational radiation [4, 5]. This is in contrast to Newtonian gravity where bodies can follow closed, elliptical orbits [6, 7]. As the binary shrinks, the frequency and amplitude of the emitted GWs increase. Eventually the two objects merge. If these objects are BHs, they form a single perturbed BH that radiates GWs at a constant frequency and exponentially damped amplitude as it settles to its final state [8, 9].

tational resources.

[1] B. Abbott *et al.*, Phys. Rev. Lett. **116**, 061102 (2016), https://dcc.ligo.org/LIGO-P150914/public/main.

[2] J. Aasi *et al.* (LIGO Scientific), Class.Quant.Grav. **32**, 074001 (2015), arXiv:1411.4547 [gr-qc].

[3] B. Abbott *et al.*, (2016), https://dcc.ligo.org/LIGO-P1500269/public/main.

[4] A. Einstein, Preuss. Akad. Wiss. Berlin , 688 (1916).

[5] A. Einstein, Preuss. Akad. Wiss. Berlin , 154 (1918).

[6] J. Kepler, *Astronomia nova ..., seu physica coelestis, tradita commentariis de motibus stellae martis* (1609).

[7] I. Newton, *Philosophiae Naturalis Principia Mathematica*

Imagen: Abbott y col. (2016, , pp. 1 y 9)

Las figuras aparecen fuera del texto cerca de su llamada

properties of space-time in the strong-field, high-velocity regime and confirm predictions of general relativity for the nonlinear dynamics of highly disturbed black holes.

II. OBSERVATION

On September 14, 2015 at 09:50:45 UTC, the LIGO Hanford, WA, and Livingston, LA, observatories detected the coincident signal GW150914 shown in Fig. 1. The initial detection was made by low-latency searches for generic gravitational-wave transients [41] and was reported within three minutes of data acquisition [43]. Subsequently, matched-filter analyses that use relativistic models of compact binary waveforms [44] recovered GW150914 as the most significant event from each detector for the observations reported here. Occurring within the 10-ms intersite

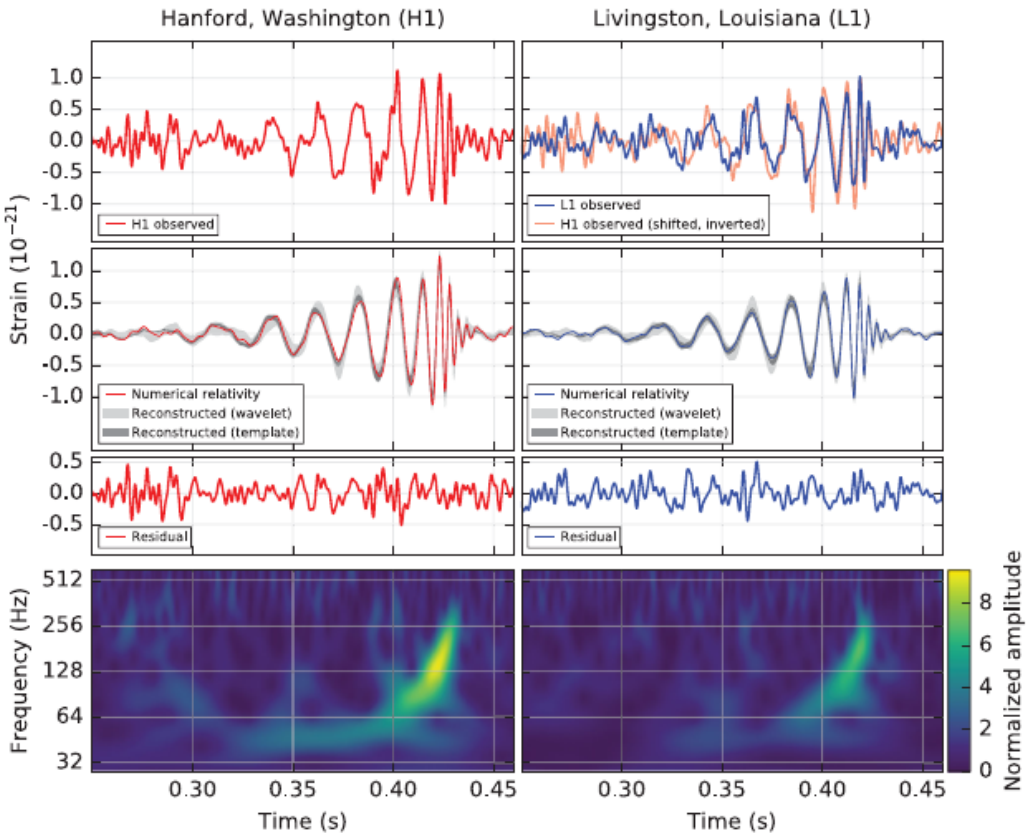

FIG. 1. The gravitational-wave event GW150914 observed by the LIGO Hanford (H1, left column panels) and Livingston (L1, right

Imagen: Abbott y col. (2016, http://bit.ly/1UQoCsR, p 2)

Figura 3.5.1: Ejemplo de figura y llamada a figura.[3] Habitualmente las figuras y cuadros aparecen siempre numerados y con una llamada dentro del texto: no son elementos ajenos.

Las fórmulas aparecen «en línea» y pueden numerarse o no

and is a periodic function as discussed previously. For multi-GeV x-ray FELs the undulator focusing term is weak and to a good approximation the external focusing dominates. The solutions for the betatron equations can then be written in the form of Eq. (2.16).

The oscillations described by Eqs. (2.33) and (2.34) are called betatron oscillations. Their wave number,

$$\beta_{B,F} = 1/\sqrt{\Omega_{\text{ext}}^2 + \Omega_{\text{und}}^2}, \tag{2.38}$$

is used to measure the strength of the beam focusing in the undulator.

For an ensemble of particles executing betatron oscillations, and neglecting effects like particle-particle scattering and dissipative forces, the volume in the six-dimensional phase space of coordinates (x, y, p_x, p_y, z, and p_z) is conserved. In our approximation of small transverse momenta we can write, using the angle of the momentum with respect to the undulator axis, $p_{x,y} = mc\gamma\theta_{x,y}$. For uncoupled motion in the three coordinates and constant beam energy, there are three separate invariants, proportional to the areas in the planes $(x, \gamma\theta_x)$ or $(y, \gamma\theta_x)$, for the transverse coordinates and $(z,\ p_z)$. These invariants are called the transverse and longitudinal normalized beam emittance $\varepsilon_{N,x,y}$ and $\varepsilon_{N,L}$ defined as

$$\beta_{x0} = -(K/\gamma)\sin(k_U z), \tag{2.44}$$

$$\beta_{y0} = 0, \tag{2.45}$$

$$\beta_{z0} = 1 - \{1 + (K^2/2)[1 - \cos(2k_U z)]\}/2\gamma^2. \tag{2.46}$$

The main difference between the helical and the planar undulator case appears in the longitudinal velocity, a constant in the first case, and modulated at twice the undulator periodicity in the second case. This modulation introduces in the radiation spectrum on axis all odd harmonics of the fundamental frequency, absent in the helical case, as seen in Secs. II.F and II.H.

To obtain the position along the undulator as a function of time we integrate Eq. (2.46) and obtain an approximate solution, to order $1/\gamma^4$,

$$z = \bar{\beta}_o ct - S_p \sin(2k_U \bar{\beta}_o ct), \tag{2.47}$$

where

$$\bar{\beta}_o = 1 - (1 + K^2/2)/2\gamma^2 \tag{2.48}$$

is the average longitudinal velocity over an undulator period, and $S_p = K^2/(8k_U\bar{\beta}_o\gamma^2)$.

Imagen: Pellegrini, Marinelli y Reiche (2016, http://bit.ly/1ZGfgzA, p. 8)

Figura 3.5.2: Ejemplo de ecuaciones numeradas y de llamada a una ecuación.[6] Convienen numerar todas las ecuaciones incluso cuando no vayan a ser llamadas.

Índice

Bibliografía y citas I

[1] Isaac Newton. *Philosophiae naturalis principia mathematica*. J. Societatis Regiae ac Typis J. Streater, 1687. URL: http://bit.ly/1ZFuAg3.

[2] Sadi Carnot. *Réflexions sur le puissance motrice du feu, et sur les machines propes á dèveloper cette puissance*. Bachelier, Paris, 1824.

[3] B. P. Abbott y col. «Observation of Gravitational Waves from a Binary Black Hole Merger». En: *Phys. Rev. Lett.* 116 (6 feb. de 2016), pág. 061102. DOI: 10.1103/PhysRevLett.116.061102. URL: http://bit.ly/1UQoCsR.

[4] J. H. Taylor y J. M. Weisberg. «A new test of general relativity - Gravitational radiation and the binary pulsar PSR 1913+16». En: *The Astrophysical Journal* 253 (feb. de 1982), págs. 908-920. DOI: 10.1086/159690.

[5] Rudolf Clausius. *Abhandlungen über die mechanische Wärmetheorie*. Vol. II. Braunschweig, 1867. URL: http://bit.ly/1UGjaHJ.

Bibliografía y citas II

[6] C. Pellegrini, A. Marinelli y S. Reiche. «The physics of x-ray free-electron lasers». En: *Rev. Mod. Phys.* 88 (1 mar. de 2016), pág. 015006. DOI: 10.1103/RevModPhys.88.015006. URL: http://bit.ly/1ZGfgzA.

[7] B. P. Abbott y col. *Properties of the binary black hole merger GW150914*. 2016. arXiv: 1602.03840v1 [gr-gc].

[8] Donald E. Knuth, Tracy Larrabee y Paul M. Roberts. *Mathematical Writing*. Inf. téc. Standford University, 1987. URL: http://bit.ly/1UwxpAU.

[9] Academia Obscura (@AcademiaObscura). Tweet. 24 de mar. de 2016. URL: http://bit.ly/22H2q9C.

[10] David E. Bock, Paul Velleman y Richard D. De Veaux. *Stats: Modeling the World*. 4th. Pearson, 2014. ISBN: 978-0321854018.

[11] Maria Paz Garcia Sanz y Pilar Martinez Clares. *Guia práctica para la realización de trabajos fin de grado y trabajos fin de master*. Editum (Universidad de Murcia), 2012. ISBN: 978-8483719732.

Bibliografía y citas III

[12] Juana María González García, Ana León Mejía y Mercedes Peñalba Sotorrío. *Cómo escribir un trabajo de fin de grado*. Síntesis, 2014. ISBN: 978-8490770481.

[13] Melissa Walker. *Cómo escribir trabajos de investigación (Herramientas Universitarias)*. Gedisa, 2015. ISBN: 978-8474327243.

[14] Gustavo A. Slafer. «Cómo escribir un artículo científico». En: *Revista de Investigación en Educación* 6 (2009), págs. 124-132.

[15] Claus Ascheron y Angela Kickuth. *Make your mark in Science*. John Wiley y Sons, Inc, 2005. ISBN: 0-471-65733-6.